C233/76

STABILIZATION OF TURBOMACHINERY WITH SQUEEZE FILM DAMPERS – THEORY AND APPLICATIONS

E. J. GUNTER, BSME, MSEM, PhD EM, Member ASME, L. E. BARRETT, BSME, MSME,
and
P. E. ALLAIRE, BEME, MEME, PhD ME
University of Virginia, Charlottesville, Virginia USA

The MS of this paper was received at the Institution on 30 March 1976 and accepted for publication on 18 June 1976

SYNOPSIS This study investigates the steady-state and transient response of the squeeze film damper bearing. Both the steady-state and transient equations for the hydrodynamic bearing forces are derived. The steady-state equations are used to determine the damper equivalent stiffness and damping coefficients. The coefficients are used to find the damper configuration which will provide the optimum support characteristics based on a stability analysis of the rotor-bearing system. The effects of end seals and cavitated fluid film are included. The transient analysis of rotor-bearing systems is performed by coupling the damper and rotor equations and integrating forward in time. The effects of unbalance, bearing cavitation and retainer springs, aerodynamic forces, and internal friction damping are included in the analysis. Particular emphasis is placed on solving the system characteristic frequency equation, and stability maps produced using this method are presented. The study shows that for optimum stability and low force transmissibility the squeeze bearing should operate at an eccentricity ratio of $\varepsilon < 0.4$. Experimental data is presented showing the elimination of instability in a ten-stage centrifugal compressor by the use of squeeze film dampers.

1. INTRODUCTION

Modern turbomachines are highly complex systems. Current design trends are producing machines that consist of several process stages joined together. The rotors in these machines are highly flexible shafts, often mounted in more than two bearings, that rotate at very high speeds. It is not uncommon to see machines that operate above the second critical speed. As a result the system dynamics are very complicated.

One of the major problems encountered in these machines is instability produced by aerodynamic forces on impeller wheels, friction in the stressed rotor and hydrodynamic forces in the bearings. The instability is characterised by large amplitude, nonsynchronous whirl orbits and often results in bearing or total machine failure. It is often aggravated by seals and external forces transmitted to the machine.

From the earliest investigations of rotor instability, it has been known that the use of flexible, damped supports has an effect on instability and can eliminate it or alter the speed at which it occurs. The squeeze film damper bearing is one type of flexible support that is currently being investigated. This study examines the squeeze bearing and through computer simulation shows its effects on several rotor-bearing systems. The equations for the hydrodynamic damper forces are developed in both fixed and rotating coordinate systems. The use of two coordinate systems allows for both steady-state and transient analysis of damper performance.

The steady-state behavior of the damper results in the formulation of damper stiffness and damping coefficients which can be used to size the damper configuration. This is accomplished by comparing the coefficients with required values obtained from a stability analysis of the rotor-bearing system.

The transient analysis is very useful in determining the response to particular forms of external and internal forces as noted previously. Also the effect of damper retainer springs and fluid film cavitation can be found. The transient response is found by tracking the journal motion forward in time by integrating the equations of motion under the influence of the system forces.

2. NOTATION

c	Bearing clearance
C_o	Equivalent damper bearing damping coefficient
C_{xx}, C_{xy} C_{yy}, C_{yx}	Bearing damping coefficient
e, ε	Journal eccentricity ($\varepsilon = e/c$)
e_u	Mass unbalance eccentricity
EMU	Ratio of unbalance eccentricity to bearing clearance, e_u/c
F_x	Force component in x-direction
F_y	Force component in y-direction
F_r	Force component in radial direction
F_θ	Force component in tangential direction
FMAX	Maximum hydrodynamic force
FU	Force due to rotating unbalance, $me_u\omega^2$
FURATIO, TRD	Ratio of FMAX to FU
h	Fluid film thickness

K_o	Equivalent damper bearing stiffness coefficient
KRX, KRY	Retainer spring stiffness coefficient
K_{xx}, K_{xy} K_{yy}, K_{yx}	Bearing stiffness coefficient
L	Bearing length
m	Journal mass
N	Rotor speed
P	Pressure
PMAX	Maximum hydrodynamic pressure
Q	Aerodynamic cross-coupling coefficient
R	Bearing radius
t	Time
W	Weight
x, y, z	Displacements
μ	Dynamic viscosity
θ, θ'	Angular measure
$\dot{\phi}$	Journal precession rate
ω	Angular velocity

3. THEORETICAL ANALYSIS

3.1. Reynolds equation

The configuration of the squeeze film damper bearing is shown in Fig. 1 where the clearance has been exaggerated. Both fixed and rotating coordinate systems are shown.

The basic bearing equation is the Reynolds equation which is derived from the Navier-Stokes equations for incompressible flow. With the proper bearing parameters the equation for the fluid film forces are derived (1)*. The short bearing approximation is used since most dampers have a low L/D ratio (2).

The Reynolds equation for the short, plain journal bearing is given in both fixed coordinates by:

$$\frac{\partial}{\partial Z}\left[\frac{h^3}{6\mu}\frac{\partial P}{\partial Z}\right] = \left(\omega_b + \omega_j\right)\frac{\partial h}{\partial \theta} + 2\frac{\partial h}{\partial t} \qquad (1)$$

In the fixed coordinate system the film thickness, h, is given by:

$$h = c - x\cos\theta - y\sin\theta \qquad (2)$$

Substituting into Equation (1) and integrating yields:

$$P(\theta, Z) = \frac{3\mu}{h^3}\left[Z^2 - LZ\right]\left[\left(\omega_b + \omega_j\right)\frac{\partial h}{\partial \theta} + 2\frac{\partial h}{\partial t}\right] \qquad (3)$$

*References are given in the Appendix.

3.2. Bearing forces in fixed coordinates

The total force components in the x and y directions are found by integrating the pressure over the entire journal surface.

For the case of the squeeze film damper where the journal and housing are constrained from rotating, $(\omega_b = \omega_j = 0)$, the force expression becomes

$$\begin{Bmatrix} F_x \\ F_y \end{Bmatrix} = \frac{-\mu R L^3}{2}\int_0^{2\pi} \frac{-2(\dot{x}\cos\theta + \dot{y}\sin\theta)}{(c - x\cos\theta - y\sin\theta)^3}\begin{Bmatrix}\cos\theta \\ \sin\theta\end{Bmatrix} d\theta \qquad (4)$$

The nonlinear fluid film forces are easily combined with the rotor-bearing system dynamical equations providing a complete nonlinear dynamical analysis of the system. Because the bearing force equations are written in fixed Cartesian coordinates, a transformation from one coordinate system to another is not required. This is very important for conservation of computation time since the bearing pressure profile must be integrated at each time step of the system motion.

3.3. Bearing forces in rotating coordinates

If the Reynolds equation is written in polar coordinates, it may be integrated in closed form assuming steady-state circular precession of the journal about the bearing centre and no axial misalignment. The resulting equations for the bearing forces give the equivalent stiffness and damping of the bearing.

The force components are:

$$\begin{Bmatrix} F_r \\ F_\theta \end{Bmatrix} = \frac{-\mu R L^3}{c^2}\int_{\theta_1'}^{\theta_2'} \frac{(\dot{\phi}\,\varepsilon\sin\phi' + \dot{\varepsilon}\cos\phi')}{(1 + \varepsilon\cos\phi')^3}\begin{Bmatrix}\cos\theta' \\ \sin\theta'\end{Bmatrix} d\theta' \qquad (5)$$

The limits of integration, θ_1' and θ_2', define the area over which a positive pressure profile exists and are dependent on the type of journal motion and whether or not cavitation occurs.

It is assumed that the damper is precessing in steady-state circular motion about the origin and therefore $\dot{\varepsilon} = 0$.

The resulting force components are:

$$F_r = \frac{-2\mu R L^3 \varepsilon\omega e}{c^3(1 - \varepsilon^2)^2} \qquad (6)$$

and

$$F_\theta = \frac{-\mu R L^3 \pi e\omega}{2c^3(1 - \varepsilon^2)^{3/2}} \qquad (7)$$

The force in equation (6) appears as a stiffness coefficient times a displacement acting in line of the displacement towards the bearing centre. The equivalent damper stiffness is:

$$K_o = \frac{2\mu R L^3 \varepsilon\omega}{c^3(1 - \varepsilon^2)^2} \qquad (8)$$

Since the journal is precessing and not rotating, every point in the journal has a velocity equal to $e\omega$. The force in equation (7) therefore appears as a damping coefficient times a velocity acting in the direction opposite the journal motion.

The equivalent damping coefficient is:

$$C_o = \frac{\mu R L^3 \pi}{2c^3(1 - \varepsilon^2)^{3/2}} \qquad (9)$$

For the uncavitated film, the components are given by:

$$F_r = 0$$

$$F_r = \frac{-\mu R L^3 \pi e \omega}{c^3(1 - \varepsilon^2)^{3/2}} \qquad (10)$$

It is therefore evident that a complete fluid film does not produce an equivalent bearing stiffness, but doubles the damping of the cavitated film.

Although the equations for the damper characteristics were derived for a plain damper, they are applicable to other damper configurations such as a damper with a circumferential oil groove and full end leakage, or one which has a circumferential oil groove and end seals to prevent end leakage.

The damper equations derived in this section are summarized in Table 1. Also included in the table are the equations for pure radial squeeze motion. For this type of operation $\phi = 0$, and it results from a purely unidirectional load on the journal. The radial and tangential force components are derived from equation (5) where only the term containing ε in the integral is retained. The pressure equation is also modified to include only the ε term. The maximum pressure occurs at $\theta' = \pi$ for all values of journal eccentricity. Examination of the pressure equation reveals that the hydrodynamic pressure is positive only in the region $\theta' = \frac{\pi}{2}$ to $\frac{3\pi}{2}$. These values of θ' are the limits of integration in equation (5) for the cavitated film.

The table also shows that for purely radial motion no damper stiffness is obtained in either the cavitated or uncavitated damper. Thus if this type of motion exists, retainer springs must be included to provide support flexibility.

For the case of circular damper precession, the table shows the damping of the cavitated and the uncavitated film remains essentially constant for low eccentricity ratios. As the eccentricity ratio increases above 0.4, there is a rapid increase in both stiffness and damping, and they approach infinity as ε approaches 1. This variation of stiffness in the cavitated film is very important. As the eccentricity becomes large, the support becomes more rigid with a corresponding increase in the rotor critical speed. If the rotor critical speed is increased above the operating speed, the phase angle between the rotor unbalance vector and amplitude vector becomes less than 90°. When this condition occurs, the force transmitted through the support structure will always be greater than the unbalance load. With an uncavitated film, this problem does not occur because no damper stiffness is generated. To obtain the stiffness required to stabilize a rotor, it is necessary to use retainer springs in the support bearings.

4. ROTOR-BEARING STABILITY AND DAMPER ANALYSIS

4.1. Rotor-bearing stability

Many investigations into the causes of rotor-bearing instability have been performed (3-13). Also a number of methods of determining rotor-bearing system stability have been developed.

One of the most general methods for determining rotor stability is to derive the characteristic frequency equation of the system. The stability is given by the roots of this equation. The real part of the root corresponds to an exponentially increasing or decreasing function of time. Thus a positive real part indicates instability whereas a negative real part indicates a stable system. This type of stability analysis of a rotor-bearing system therefore requires that the characteristic equation be known. This equation is not always easy to obtain.

The characteristic equation is derived from the homogeneous second order differential equations of motion of the system (13). By assuming solutions of the form

$$x_i = A_i e^{\lambda t} \qquad i = 1, 2, \ldots, n$$

and differentiating, the equations are substituted back into the equations of motion. This produces a matrix know as the characteristic matrix. The determinant of this matrix gives the characteristic equation, a polynomial of degrees $2n$ in λ, where n is the number of degrees of freedom of the system.

A typical rotor-bearing system is shown in Fig. 2. The rotor is assumed to remain stationary in the axial direction so the rotor has six degrees of freedom and the characteristic equation is therefore of degree twelve. The stability maps for this system were produced with linearized journal and support bearing characteristics. The assumption of linear bearing characteristics is useful because for low eccentricity ratios the characteristics do not vary greatly with changes in eccentricity.

The system parameters are

Rotor Weight	W2	=	3,002.4 N (675.0 lb)
Journal Weight	WJ	=	1,387.8 N (312.0 lb) (each)
Support Weight	W1	=	66.7 N (15.0 lb) each
Shaft Stiffness	KS	=	490,330 N/cm (280,000 lb/in)
Shaft Damping	CS	=	0.18 N-sec/cm (0.10 lb-sec/in)
Internal Damping	CI	=	0.0 N-sec/cm
Rotor Speed	N	=	10,000 rev/min

$K_{xx} = 2.254 \times 10^6$ N/cm (1.287×10^5 lb/in)

$K_{yy} = 2.501 \times 10^6$ N/cm (1.428×10^5 lb/in)

$C_{xx} = 2{,}101$ N-sec/cm (1,200 lb-sec/in)

$C_{yy} = 2{,}259$ N-sec/cm (1,290 lb-sec/in)

$K_{xy} = K_{yx} = 0.0$ N/cm

$C_{xy} = C_{yx} = 0.0$ N-sec/cm

Two values of aerodynamic cross coupling were selected, Q = 35,023.6 N/cm (20,000 lb/in) and Q = 175,118 N/cm (100,000 lb/in). For each

value of Q, several values of support stiffness were selected ranging from 87,559 N/cm (50,000 lb/in) to 875,590 N/cm (500,000 lb/in). For each value of support stiffness a range of support damping values from 0 to 17,512 N-sec/cm (0 - 10,000 lb-sec/in) was used. Using this method a stability contour is found for a given value of aerodynamic cross-coupling and support stiffness. The rotor and bearing characteristics remained unchanged.

Figs. 3 and 4 show the stability maps for the above system for the two values of aerodynamic cross-coupling. There is an intermediate range of support damping values for which the system is stable for a given value of the support stiffness. As the stiffness is increased the system becomes less stable. With Q = 35,024 N/cm (20,000 lb/in) the optimum amount of damping ranges from 876 to 4,378 N-sec/cm (500 to 2,500 lb-sec/in) as the stiffness increases from 87,559 to 875,590 N/cm (50,000 to 500,000 lb/in). For damping less than 175.1 N-sec/cm (100 lb-sec/in) the system is unstable for all values of stiffness. The same is true if the damping exceeds 17,512 N-sec/cm (10,000 lb-sec/in).

For Q = 175,118 N/cm (100,000 lb/in) the optimum damping is 1,751 N-sec/cm (1,000 lb-sec/in) and does not shift over the stiffness range selected. When the support stiffness reaches 437,795 N/cm (250,000 lb/in) the system is unstable for all values of damping.

4.2. Steady-state analysis

The linearized stability maps just discussed provide information on the support characteristics needed to promote stability in a given rotor-bearing system. There remains the problem of relating these characteristics to the actual damper system. The squeeze bearing equations derived in Section 2 in rotating coordinates are used to determine the preliminary bearing design.

The damper characteristics, stiffness, damping, and pressure are functions of the amplitude of the journal orbit, fluid viscosity, and damper geometry. The addition of oil supply grooves, end seals, and cavitation affect the damper characteristics.

Figs. 5 and 6 show the characteristics for a damper being considered for the 3,002 N (675 lb) rotor system described earlier. The damper has an oil supply groove and end seals, and the fluid film is assumed to be cavitated. The damper parameters are, length 2.54 cm (1.0 in), radius 3.05 cm (1.20 in), and fluid viscosity 0.069 Pa S (1.0×10^{-5} lb-sec/in^2).

For the case where Q = 35,024 N/cm (20,000 lb/in) it was determined that the optimum support damping is about 876 N-sec/cm (500 lb-sec/in), and the support stiffness should be less than 175,118 N/cm (100,000 lb/in). Because it is desirable to keep the eccentricity ratio of the damper low, Figs. 5 and 6 reveal that this damper will provide the necessary stiffness and damping characteristics with a clearance of about 0.102 mm (0.004 in) at an eccentricity ratio of ε = 0.10 to 0.20. This corresponds to a damper orbit of 0.010 to 0.020 mm (0.0004 to 0.0008 in) amplitude. The maximum hydrodynamic pressure in the damper is about 0.689 M Pa (100 lb/in^2) for this clearance. If the fluid film does not cavitate, the resulting damping characteristics are doubled. A slightly larger clearance, 0.127 mm (0.005 in) will produce the optimum damping. However, because the uncavitated film does not produce an equivalent stiffness, retainer springs must be incorporated in the damper. If the end seals are flexible, the required spring rate may be obtained from them.

One advantage of the uncavitated film is that if the journal eccentricity ratio should become very large, there is no rise in stiffness that could cause the system to become unstable or raise the critical speed above the operating speed.

If Q = 175,118 N/cm (100,000 lb/in), the optimum damping is 1,752 N-sec/cm (1,000 lb-sec/in) and the effective damper stiffness developed by the combination of the retainer spring support and the damper hydrodynamic action cannot exceed 175,118 N/cm (100,000 lb/in). In order to achieve the necessary damping required, a low clearance damper of the order of 0.076 to 0.102 mm (0.003 to 0.004 in) is needed. However, since the total support stiffness cannot exceed 175,118 N/cm (100,000 lb/in) then with a 0.076 mm (0.003 in) clearance, the eccentricity of the damper cannot exceed 0.0038 mm (0.00015 in). With a 0.076 mm (0.003 in) clearance and the damper operating with a synchronous orbit of ε = 0.23 about the damper centre, a stiffness of 437,795 N/cm (250,000 lb/in) will be generated. This high value of stiffness therefore will prevent the rotor system from achieving stabilization.

If the aerodynamic cross-coupling on the machine is 175,118 N/cm (100,000 lb/in), then the squeeze film damper must be sized very carefully for the application because of the large aerodynamic loading on the machine. For example, in Fig. 6, a line is drawn at the stiffness value of 175,118 N/cm (100,000 lb/in). The damper cannot be operating above this level because of the excessive stiffness that would be generated by the damper. The intersection of this stiffness value with the clearance curves of 0.076, 0.156, and 0.254 mm (0.003, 0.006, and 0.010 in) produces the maximum allowable operating eccentricity for this design of damper. In Fig. 5 the line of 2,627 N-sec/cm (1,500 lb-sec/in) is drawn on the figure. The operation of the damper cannot be above this level as this would produce excessive damping in the system. Likewise the line at 613 N-sec/cm (350 lb-sec/in) is drawn on the figure, and the damper cannot operate below this limit as there would be insufficient damping produced in order to stabilize the rotor. Thus the damper must operate so as to produce a range of damping coefficients between 613 and 2,627 N-sec/cm (350 - 1,500 lb-sec/in) if the rotor is to be stabilized with this high value of aerodynamic cross-coupling. Next the points of intersection from Fig. 6 where the stiffness line of 175,118 N/cm (100,000 lb/in) intersects the clearance curve is superimposed on Fig. 5 and this line is drawn. The operation above this line will produce excessive stiffness in the damper. The region bounded by the excessive stiffness line and the damping lines produces the allowable design region. For this case of damper under consideration, it can be seen that there is only a small allowable design region between 0.063 to 0.102 mm (0.0025 to 0.004 in) bearing clearance with a maximum eccentricity ratio of 0.2. If the damper does not operate in this region, then proper stabilization of the rotor configuration will not be achieved. If the damper system is to be designed to stabilize a Q value of 175,118 N/cm (100,000 lb/in), it is therefore desirable to study other damper lengths and clearance values in order to obtain a damper

configuration which has a larger design region. If the Q value for design is only required to be 35,024 N/cm (20,000 lb/in), then the design region is greatly extended, and the permissible damper clearance can vary from 0.076 to 0.152 mm (0.003 to 0.006 in) with a maximum eccentricity ratio of 2.6.

5. ROTOR TRANSIENT ANALYSIS

In the previous section, the design characteristics of the damper were presented based upon linearized bearing theory. It is often important to evaluate the rotor dynamical behaviour with and without a squeeze film damper under operating conditions. In order to gain an understanding of the type of rotor motion generated in the system under the action of aerodynamic cross-coupling or internal rotor friction, the rotor system previously presented was run with a transient programme to simulate the motion at the rotor centre and the bearing locations.

Fig. 7 represents the rotor centre motion of a turborotor mounted in tilting pad bearings operating at 10,000 rev/min. The rotor mass centre has a small unbalance eccentricity of 0.0127 mm (0.0005 in). The rotor is operating with an internal friction damping of 35 N-sec/cm (20 lb-sec/in). The behaviour of the rotor is similar to the case where Q equals 35,024 N/cm (20,000 lb/in).

If noncontacting probes were placed at the rotor centre, a large whirl orbit of over 0.102 mm (0.004) would be detected as shown in Fig. 7. If the rotor speed increases while the aerodynamic cross-coupling or internal friction remains constant, then the whirl amplitude will greatly increase. Sustained rotor operations under these conditions could result in the contacting of the rotating element with the casing with possible dire consequences.

Fig. 8 represents the rotor system with a squeeze damper support system added to it with a design support stiffness of 227,654 N/cm (130,000 lb/in) and a support damping of 263 N-sec/in (150 lb-sec/in). The rotor system is released, and the centreline rapidly spirals out from the origin due to the application of the rotor unbalance. After approximately 10 cycles of shaft motion, the initial transient motion dies out, and the rotor assumes a stable synchronous whirl orbit with a maximum amplitude of 0.0254 mm (0.001 in). Fig. 9 represents the rotor motion with the speed increased to 16,000 rev/min. The absolute rotor orbit shown in the figure represents the trajectory from 10 to 18 cycles of shaft motion. Here again it can be seen that the rotor is approaching a highly stable synchronous whirl orbit. In Figs. 8 and 9 it is seen that the rotor, under the action of low internal friction or aerodynamic cross-coupling, can be stabilized with a damping value as low as 263 N-sec/cm (150 lb-sec/in). However, if the damping value chosen for the damper is too low, the rotor is unstable.

The transient rotor and damper motion presented in the previous figures was based upon linearized bearing and damper coefficients. In the actual damper, the forces generated are highly nonlinear functions of the journal displacement and velocity components. In order to take this into consideration, transient orbits of the rotor bearing system were run using the complete nonlinear damper forces in the computer programme. It has been found that the unbalance level, alignment, and the magnitude of the retainer spring rate have a significant effect on the ability of the damper to perform properly. For example, Fig. 10 represents the motion of the squeeze film damper with a retainer spring of 87,559 N/cm (50,000 lb/in) and a clearance of 0.178 mm (0.007 in). The rotor has a mass unbalance eccentricity, e_u, of 0.045 mm (0.00175 in), which creates a rotating load of 16,458 N (3,700 lb). Although the initial starting position assumed was considerably removed from the final steady-state orbit, it can be seen that the initial transient quickly dies out and the damper assumes a synchronous circular orbit with an eccentricity of radius of 0.25. The maximum dynamic transmissibility, TRD, encountered was 0.74 which occurred during the first cycle of shaft motion. After the steady state motion is achieved, the final dynamic transmissibility is greatly reduced and is of the order of 0.37. Therefore it can be seen that the squeeze film damper, in addition to stabilizing the rotor motion also greatly assists in the attenuation of the forces generated by rotor unbalance.

6. EXPERIMENTAL ROTOR MOTION

The squeeze film damper bearing has been applied successfully to several centrifugal compressors in order to stabilize them from self-excited whirl motion. However in each case, the squeeze film damper bearing had to be carefully sized for the particular machine in consideration. The design of the squeeze film damper for one machine may not necessarily produce satisfactory results in another. Fig. 11 represents a centrifugal compressor before and after stabilization with a squeeze film damper. The trace at the left represents the original orbit of the rotor operating at a compressor discharge pressure of 1.21 MPa (175 lb/in^2). The rotor became highly unstable above this discharge of pressure. After the squeeze film damper was employed, the full compressor discharge pressure could be achieved. The resulting whirl orbit as shown in the right hand upper figure shows that the rotor system is highly stable with only a small component of self-excited whirl motion existing in the rotor.

Fig. 12 represents the frequency spectrum for various operating speeds of a 10-stage centrifugal compressor in tilting pad bearings which exhibited whirl instability at the design operating speed of 13,500 rev/min. The rotor was run from 0 to 14,000 rev/min, and the motion was recorded on tape and analyzed through a real time analyzer. At the various speeds, an analysis was made of the frequency components of the rotor motion. For example, the 45° line drawn on the plot represents the synchronous rotor motion. There is also a small component at twice the operating speed as seen on the chart. At a rotor speed of 10,500 rev/min, a small component of self-excited whirl instability was detected. The frequency of this component corresponds approximately to the first critical speed at 4,200 rev/min. As the speed of the rotor is increased, the subsynchronous whirl motion grows. Operation under these conditions caused a considerable wearing of the seals and bearings and periodic replacement of these components was required.

Squeeze film dampers were designed for this compressor using the methods developed in the previous sections. Fig. 13 represents the

frequency spectrum of the compressor with the squeeze film dampers installed. Note that the rotor system is now highly stable and that there is no indication of self-excited whirl instability. The synchronous motion at design speed was also reduced considerably by means of trim balancing at the coupling. It should be noted that there is no way that balancing the rotor alone could reduce or remove the self-excited nonsynchronous component in the rotor. It may also be of interest to note that the two times running speed component has not been reduced by the squeeze film dampers or by balancing the rotor. It may well be that the two times component is caused by a misaligned coupling, and that a hot alignment should be performed on the machine.

Oscilloscope traces of the rotor orbits before and after stabilization are shown in Fig. 14. Fig. 14a shows that the total motion includes both synchronous and nonsynchronous components of vibration at the operating speed of 13,500 rev/min. Following stabilization of the rotor with dampers, Fig. 14b shows nonsynchronous motion on the upper trace and total motion on the lower trace. The resulting total motion is nearly all synchronous because the nonsynchronous component is very small.

The history of this compressor over a period of years showed slowly increasing vibration levels following each replacement of seals and bearings until wear became excessive. No large vibrations, either synchronous or nonsynchronous, were observed in the rotor operation over a one year period after the dampers were installed.

7. CONCLUSIONS

(1) Self excited whirl motion may be created in turbomachinery by one or more of the following effects: aerodynamic cross-coupling, internal friction, fluid film bearings and seals, balance pistons, and labyrinths.

(2) The use of tilting pad bearings does not guarantee stable operation because of other effects as mentioned above.

(3) Long multi-stage turborotors operating at several times the rotor first critical speed may be very susceptible to self-excited whirl instability.

(4) With short rigid rotors, stability may be improved by a reduction of clearance of the tilting pad bearings, whereas with long flexible rotors, a reduction of bearing clearance can lead to catastrophic failure.

(5) Stability may be improved by the following:

- (a) Reduction in operating speed or power level
- (b) Reduction of instability mechanisms
- (c) Increase in effective shaft stiffness
- (d) Increase in effective rotor modal damping

(6) Properly designed squeeze film dampers can improve stability and unbalance response characteristics of turbomachinery by increasing the modal damping.

(7) The damper characteristics must be sized for a particular rotor-bearing system.

(8) For a given damper design there is a limit to the level of self-excitation that it can stabilize.

(9) The higher the level of aerodynamic cross-coupling or other self excitation the more carefully the damper must be tuned to the rotor.

(10) Excessive squeeze film stiffness or damping will reduce the effectiveness of the damper.

(11) The squeeze film damper characteristics are highly nonlinear functions of the eccentricity ratio and hence the damper may not function properly under excessive loading.

APPENDIX

References

(1) Kirk, R. G. and Gunter, E. J. 'Transient journal bearing analysis.' NASA CR-1549, 1970.

(2) Gunter, E. J. 'Influence of flexibly mounted rolling element bearings on rotor response - Part I - linear analysis.' Trans. ASME. J. Lub. Tech., January 1970, pp. 59 - 75.

(3) Jeffcott, H. H. 'The lateral vibrations of loaded shafts in the neighborhood of a whirling speed . . . the effect of want of balance.' Phil. Mag. Series 6, Vol. 37, 1919, p. 304.

(4) Newkirk, B. L. 'Shaft whipping.' Gen. Elec. Rev., Vol. 27, 1924, p. 169.

(5) Kimball, A. L. 'Internal friction as a cause of shaft whirling.' Phil. Mag., Vol. 49, 1925, pp. 724-727.

(6) Newkirk, B. L. and Taylor, H. D. 'Shaft whipping due to oil action in journal bearing.' Gen. Elec. Rev., Vol. 28, 1925, pp. 559-568.

(7) Robertson, D. 'Whirling of a journal in a sleeve bearing.' Phil. Mag., Series 7, Vol. 15, 1933, pp. 113-130.

(8) Poritsky, H. 'Contribution to the theory of oil whip.' Trans. ASME, August 1953, pp. 1153 - 1161.

(9) Pinkus, O. and Sternlicht, B. Theory of hydrodynamic lubrication, McGraw Hill, New York, 1961.

(10) Alford, J. S. 'Protecting turbomachinery from self-excited rotor whirl.' Trans. ASME. J. Engr. for Power, Vol. 87, October 1965, pp. 333 - 344.

(11) Kirk, R. G. and Gunter, E. J. 'The influence of damper supports on the dynamic response of a single mass flexible rotor - Part I: linear systems.' Report No. ME-4040-105-71U, Research Laboratories for Engineering Sciences, Dept. of Mechanical Engineering, University of Virginia, Charlottesville, VA, for NASA Lewis Research Center, March 1971.

(12) Gunter, E. J. 'Dynamic stability of rotor-bearing systems.' NASA SP-113, 1966.

(13) Choudhury, P. De. 'Dynamic stability of flexible rotor-bearing systems.' Ph.D Dissertation, University of Virginia, June 1971.

TABLE 1

TYPE OF MOTION	MAXIMUM PRESSURE	EQUIVALENT DAMPING Ko (lb/in)	EQUIVALENT DAMPING Co (lb-sec/in)
CIRCULAR SYNCHRONOUS PRECESSION $\dot{\phi} = \omega,\ \dot{\varepsilon} = 0$ CAVITATED FILM	$\dfrac{-3\mu L^2\omega\varepsilon \sin\theta_m}{2c^2(1+\varepsilon\cos\theta_m)^3}$ where θ_m is given by: $(1+\varepsilon\cos\theta_m)\cos\theta_m+3\varepsilon\sin^2\theta_m=0$	$\dfrac{2\mu RL^3\varepsilon\omega}{c^3(1-\varepsilon^2)^2}$	$\dfrac{\mu RL^3}{2c^3(1-\varepsilon^2)^{3/2}}\pi$
UNCAVITATED FILM		0	$\dfrac{\mu RL^3}{c^3(1-\varepsilon^2)^{3/2}}\pi$
PURE RADIAL SQUEEZE MOTION $\dot{\phi} = 0,\ \dot{\varepsilon} \neq 0$ CAVITATED FILM	$\dfrac{-3\mu L^2\dot{\varepsilon}\cos\theta_m}{2c^2(1+\varepsilon\cos\theta_m)^3}$ $\theta_m = \pi$	0	$\dfrac{\mu RL^3[\pi-\cos^{-1}(\varepsilon)](2\varepsilon^2+1)}{c^3(1-\varepsilon^2)^{5/2}}$
UNCAVITATED FILM		0	$\dfrac{\mu RL^3\pi(2\varepsilon^2+1)}{c^3(1-\varepsilon^2)^{5/2}}$

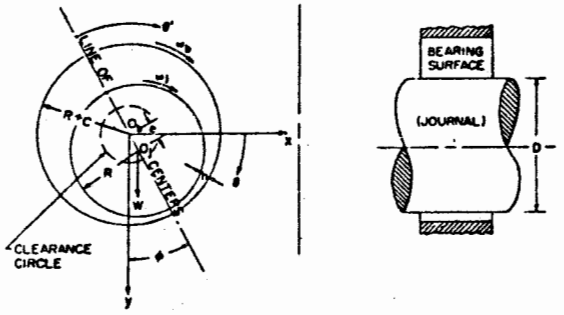

Fig. 1: Squeeze film damper bearing configuration in fixed and rotating coordinate systems

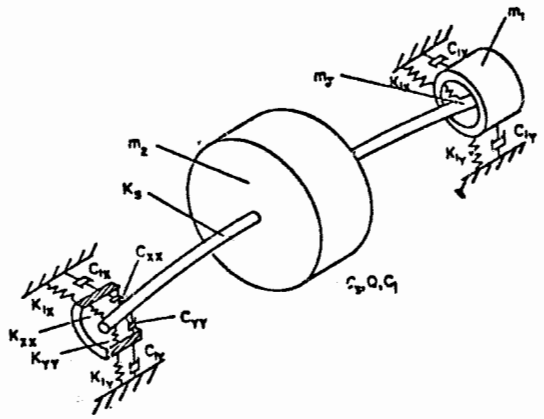

Fig. 2: Three-mass flexible rotor mounted in flexible, damped supports

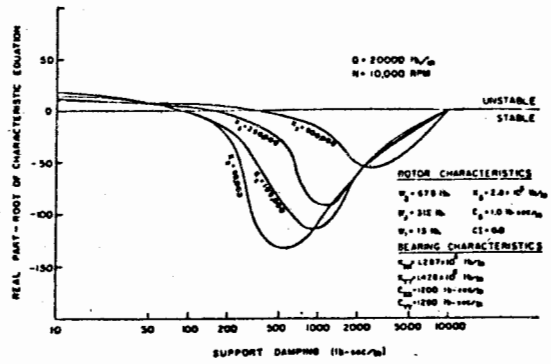

Fig. 3: Stability of a flexible rotor with aerodynamic cross-coupling, Q = 35 024 N/cm, N = 10 000 rev/min

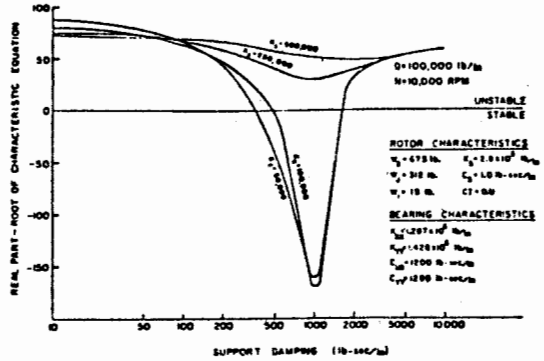

Fig. 4: Stability of a flexible rotor with aerodynamic cross-coupling, Q = 175 118 N/cm, N = 10 000 rev/min

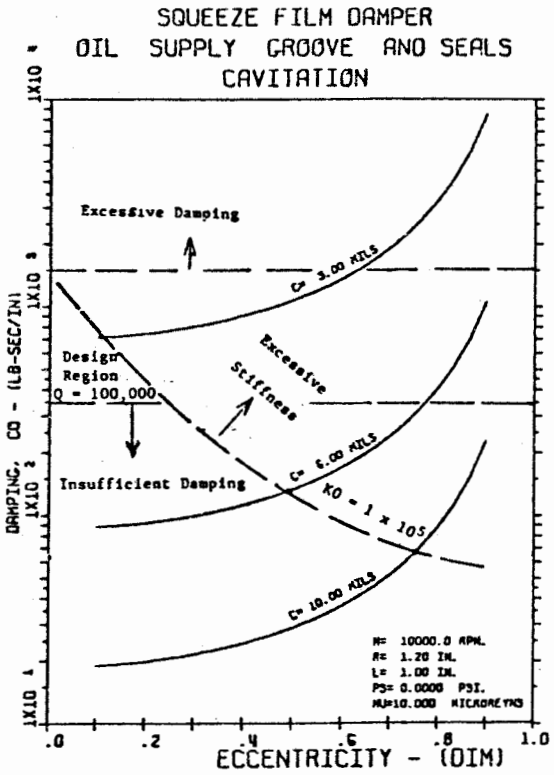

Fig. 5: Damping coefficient for squeeze film bearing with cavitated film end seals and oil supply groove included

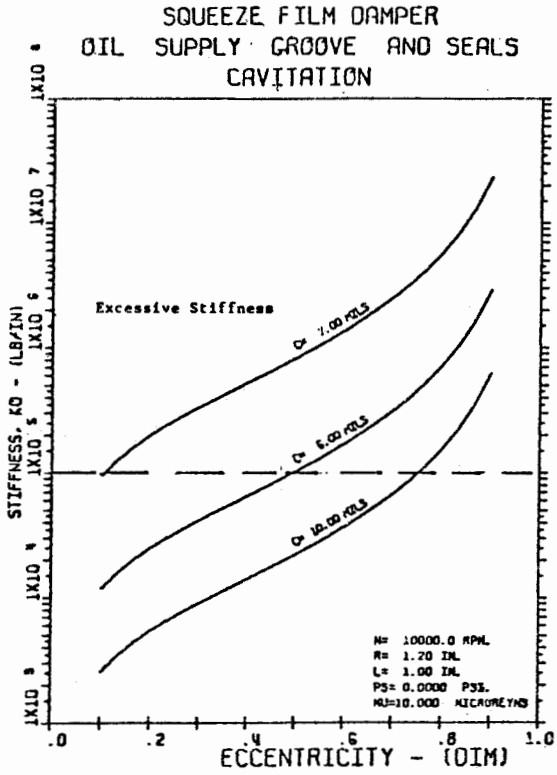

Fig. 6: Stiffness coefficient for squeeze film bearing with cavitated film end seals and oil supply groove included

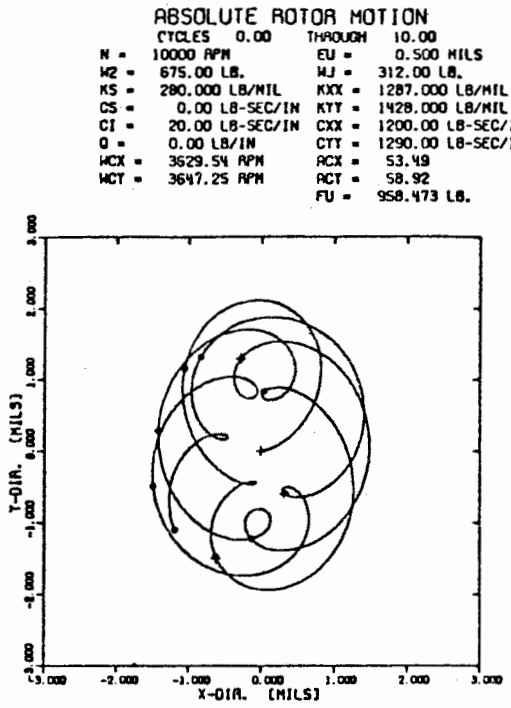

Fig. 7: Rotor centre motion at 10 000 rev/min with large self-excited motion due to internal friction, C_i = 35 N-sec/cm

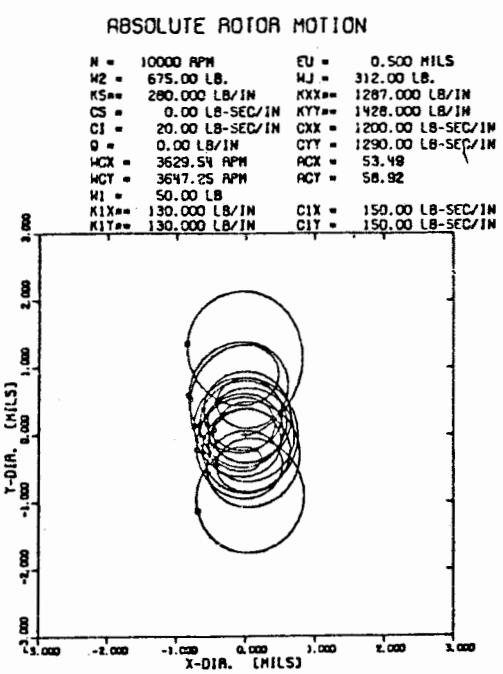

Fig. 8: Stabilized motion with damper support at 10 000 rev/min C_i = 35 N-sec/cm, K_1 = 227 554 N/cm, C_1 = 263 N-sec/cm

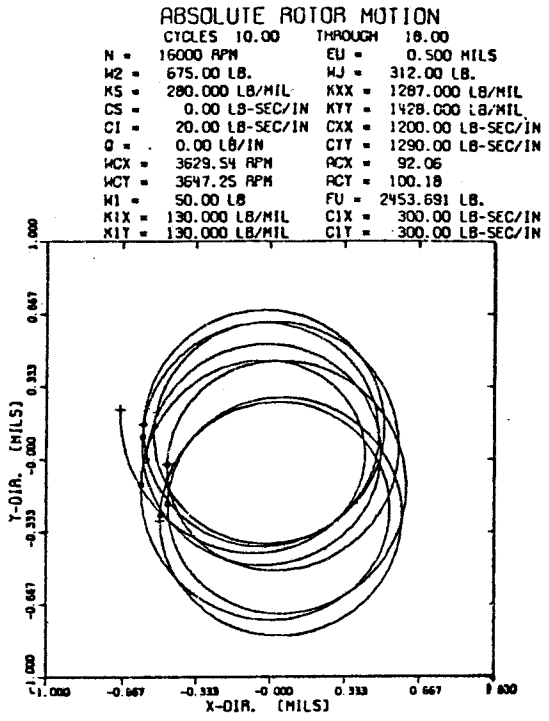

Fig. 9: Stabilized motion with damper support at 16 000 rev/min C_i = 35 N-sec/cm, K_1 = 227 654 N/cm, C_1 = 263 N-sec/cm

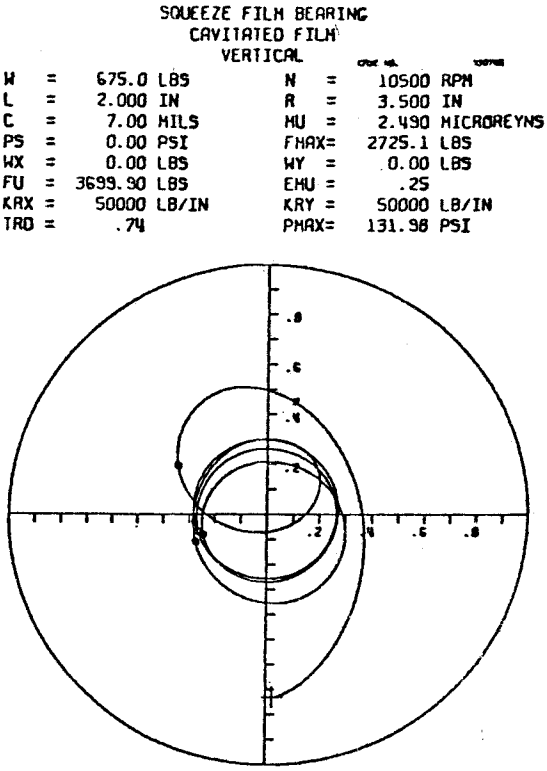

Fig. 10: Vertical unbalanced rotor in squeeze film bearing — effect of unbalanced magnitude — unbalance eccentricity — 0.045mm

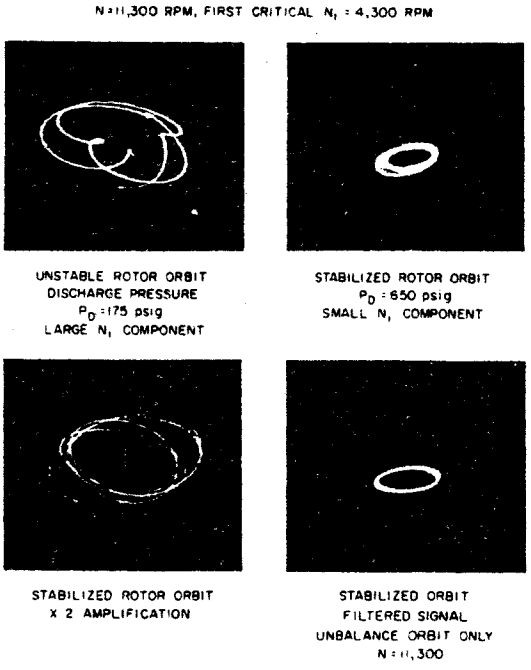

Fig. 11: Rotor orbits of a turbo compressor before and after stabilization by damper supports

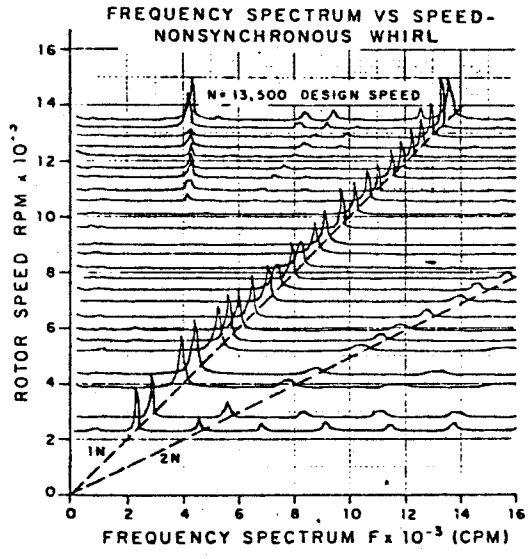

Fig. 12: Frequency spectrum vs speed — nonsynchronous whirl

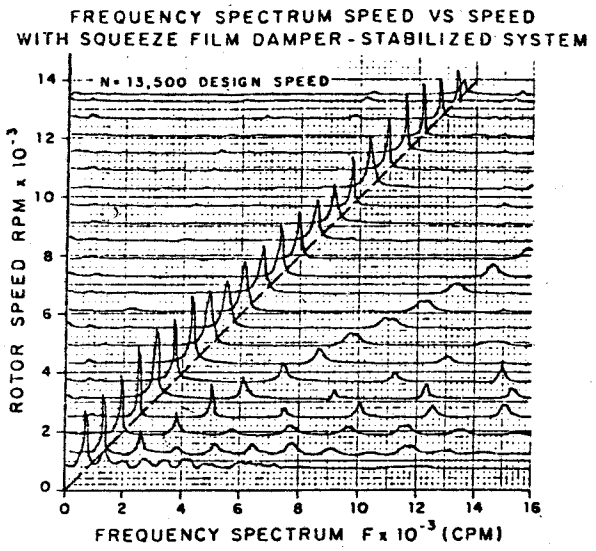

Fig. 13: Frequency spectrum speed vs speed with squeeze film dampers — stabilized system

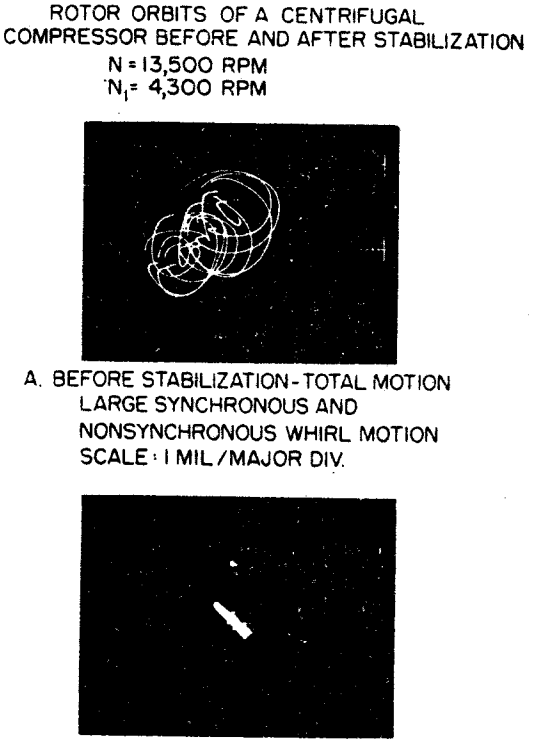

Fig. 14: Rotor orbits of a centrifugal compressor before and after stabilization,—N = 13 500 rev/min, N_1 = 4300 rev/min